Nuclear Medicine and Biology 40 (2013) 273–279

Contents lists available at SciVerse ScienceDirect

Nuclear Medicine and Biology

journal homepage: www.elsevier.com/locate/nucmedbio

Synthesis, *in vitro* and *in vivo* characterization of two novel ^{68}Ga-labelled 5-nitroimidazole derivatives as potential agents for imaging hypoxia

Soledad Fernández [a], Sylvia Dematteis [b], Javier Giglio [a,c], Hugo Cerecetto [d,*], Ana Rey [a,c,*]

[a] Cátedra de Radioquímica, Facultad de Química, Universidad de la República, Montevideo, Uruguay
[b] Cátedra de Inmunología, Facultad de Química, Universidad de la República, Montevideo, Uruguay
[c] Centro Uruguayo de Imagenología Molecular, Montevideo, Uruguay
[d] Grupo de Química Medicinal, Laboratorio de Química Orgánica, Facultad de Ciencias-Facultad de Química, Universidad de la República, Montevideo, Uruguay

ARTICLE INFO

Article history:
Received 18 September 2012
Received in revised form 29 October 2012
Accepted 1 November 2012

Keywords:
Gallium
Hypoxia
5-nitroimidazole
DOTA
Imaging agent
Complex

ABSTRACT

Introduction: Hypoxia imaging is an important field in radiopharmaceutical research since hypoxic cells are very resistant to radiation treatment and diffusional limitations restrict the efficacy of chemotherapy. Gallium-68 is a widely used radionuclide for positron emission tomography (PET) due to the availability of the ^{68}Ge/^{68}Ga-generator. With the aim to develop new potential [^{68}Ga]-radiopharmaceuticals for imaging hypoxia, we have synthesized and evaluated two novel ^{68}Ga-labelled 5-nitroimidazole derivatives.

Methods: Two 5-nitroimidazole derivatives, 10-[2-(2-methyl-5-nitro-1 *H*-imidazole-1-yl)ethylaminocarbonylmethyl]-1,4,7,10-tetraazacyclododecane-1,4,7-triacetic acid (**Nit1**) and 10-{[*N*-methyl-1-[1-(2-(2-methyl-5-nitro-1 *H*-imidazole-1-yl)ethyl)-1 *H*-1,2,3-triazole-4-yl] methylaminocarbonylmethyl}-1,4,7,10-tetraazacyclododecane-1,4,7-triacetic acid (**Nit2**) were synthesized. Preparation of [^{68}Ga]complexes [^{68}Ga]-**Nit1** and [^{68}Ga]-**Nit2** was performed at pH 4.5 and 95 °C during 15 minutes and radiochemical purity (RP) was evaluated by reverse phase HPLC. Stability, lipophilicity and plasma protein binding were studied. Biological behaviour in HCT-15 cells both in normoxia and hypoxia has been assessed. Biodistribution in animals bearing induced 3LL Lewis murine lung carcinoma was studied. Comparison with [^{18}F]FMISO is also presented.

Results: **Nit1** and **Nit2** have been successfully synthesized. Labelling in high radiochemical purity was achieved for both ligands. Complexes are stable in labelling milieu for at least four hours and in human plasma or in the presence of an excess of DTPA for at least two hours. Both compounds showed high uptake in hypoxic cells *in vitro* and a very favourable biodistribution profile in mice bearing induced tumours. Results are comparable to those obtained for [^{18}F]FMISO.

Conclusions: Selective uptake and retention in tumour together with favourable tumour/muscle ratio make these compounds promising candidates for further evaluation as potential hypoxia imaging agents.

1. Introduction

Hypoxic regions in tumours are formed when the oxygen demand of the tissue exceeds the levels provided by the bloodstream [1]. Several factors contribute to inadequate oxygen transport and hypoxia, including low vessel density and increased oxygen consumption. Angiogenesis promoted by tissue itself emerges as a strategy to meet oxygen demand. However, tumour growth often exceeds the capacity of accompanying blood vasculature to deliver adequate quantities of oxygen to the growing cell mass [2]. Clinical research has demonstrated that hypoxia has a high prevalence in advanced solid tumours [3–7] and also contributes to the progression to metastasis [8,9]. In addition, hypoxia is associated with a decrease in the effectiveness of chemotherapy due to poor diffusion of drugs from blood vessels to the tumour, and also produces increased radio-resistance due to lower concentration of free radicals from oxygen [10,11].

Due to the inherent drawbacks of invasive techniques to detect hypoxia [12], Nuclear Medicine imaging is considered an interesting alternative. Bioreductive moieties that are selectively reduced under low oxygen pressure are used in the development of potential radiopharmaceuticals with selectivity towards hypoxic tissue. The positron emission tomography (PET) tracer [^{18}F]fluoro-misonidazole (FMISO) was the first nitroimidazole used for clinical hypoxia imaging [13]. In spite of its good clinical output, [^{18}F]FMISO has been criticized because of its slow accumulation in hypoxic tumours and low tumour-to-background ratios due to non-specific binding resulting from its relatively high lipophilicity [14–16]. Other [^{18}F]-nitroimidazole derivatives have been developed such as [^{18}F]-

* Corresponding authors. Ana Rey is to be contacted in Facultad de Química at General Flores 2124, 11800 Montevideo, Uruguay. Tel.: +598 29248571; fax: +598 29241906. Hugo Cerecetto, Facultad de Ciencias, Iguá 4225, 11400 Montevideo, Uruguay. Tel.: +598 252586181; fax: +598 25250749.
E-mail addresses: hcerecet@fq.edu.uy (H. Cerecetto), arey@fq.edu.uy (A. Rey).

0969-8051/$ – see front matter © 2013 Elsevier Inc. All rights reserved.
http://dx.doi.org/10.1016/j.nucmedbio.2012.11.003

fluoroerythronitroimidazole (FETNIM), [^{18}F]-1-α-D:-(2-deoxy-2-fluoroarabinofuranosyl)-2-nitroimidazole (FAZA), [^{18}F]-2-(2-nitro-1H-imidazol-1-yl)-N-(2,2,3,3,3-pentafluoropropyl) acetamide (EF-5), and [^{18}F]-fluoroetanidazole (FETA) [17]. Although some of them, especially [^{18}F]FAZA, showed faster soft tissue clearance, none of these compounds had ideal properties and consequently [^{18}F]FMISO is still considered the gold standard for clinical hypoxic imaging. Other radionuclides have also been utilized, in particular, 68-Gallium due to its availability from a ^{68}Ge/^{68}Ga generator. Several research groups are pursuing the development of [^{68}Ga]-complexes for hypoxic tumour imaging [12,18,19]. Mukai et al. [12] reported a DOTA-derivative with two 5-nitromidazol-1-yl moieties coupled through an amide bond. Additionally, Hoigebazar et al. [18,19] developed compounds with a 2-nitroimidazol-1-yl moiety coupled to DOTA or NOTA. Some of these reported [^{68}Ga]-complexes showed moderate tumour uptake, high hidrophilicity and a fast clearance from soft tissues. Although authors claim that results obtained are comparable with those for [^{18}F]FMISO and [^{18}F]FAZA, this comparison is not made under the same experimental conditions and biological models [18]. As a consequence, it is relevant to continue developing new tracers with improved biological behaviour.

Our group has applied nitroaromatic compounds, especially nitroimidazoles and *N*-oxides to the development of potential ^{99m}Tc-radiopharmaceuticals [20–26]. The 5-nitroimidazole metronidazole has been used as starting material for their preparation with very promising results.

Consequently, we present herein the synthesis of two novel 5-nitroimidazole derivatives, 10-[2-(2-methyl-5-nitro-1 *H*-imidazole-1-yl)ethylaminocarbonylmethyl]-1,4,7,10-tetraazacyclododecane-1,4,7-triacetic acid (**Nit1**) and 10-{[*N*-methyl-1-[1-(2-(2-methyl-5-nitro-1 *H*-imidazole-1-yl)ethyl)-1 *H*-1,2,3-triazole-4yl]methylaminocarbonylmethyl}-1,4,7,10-tetraazacyclododecane-1,4,7-triacetic acid (**Nit2**) containing DOTA as chelator for ^{68}Ga and the preparation of their corresponding ^{68}Ga-complexes [^{68}Ga]-**Nit1** and [^{68}Ga]-**Nit2**. In order to assess their potentiality as hypoxia targeting radiopharmaceuticals we have studied the main physicochemical and biological properties both *in vitro* and *in vivo*.

2. Materials and methods

2.1. General

All laboratory chemicals were reagent grade and were used without further purification. Intermediates **2a** and **2b** (Scheme 1) were prepared according to a previously described procedure [24,25]. Solvents for chromatographic analysis were HPLC grade. [^{68}Ga]$GaCl_3$ was obtained from a commercial generator (Eckert & Ziegler IGG 100–50 M). Thin-layer chromatography (TLC) was carried out on pre-coated plates of silica gel 60F_{254}. For column chromatography we used silica gel (Merck, 60–230 mesh). NMR spectra were obtained at 400 MHz in the indicated deuterated solvent (Bruker DPX 400 Spectrometer). Chemical shifts are reported as δ values (parts per million) relative to TMS. Coupling constants are reported in Hertz (Hz). The multiplicity is defined by s (singlet), t (triplet), or m (multiplet). Mass spectra were registered by electronic impact (EI) on a Hewlett Packard 5973 MSD or MICROMASS (Triple Quattro) using electron impact (EI) or electrospray (ESI), respectively. IR spectra were obtained in the range 4000–200 cm^{-1} in KBr pellets at 1% in a Bomen MB – 102 FT-IR spectrometer. Melting points were determined with an electrothermal melting point apparatus (Electrothermal 9100) and were uncorrected. HPLC analysis was developed on a LC-10 AS Shimadzu Liquid Chromatography System using a reverse phase column μ-Bondapack^{TM} Waters 10 μm, C18 column (3.9 × 300 mm). Elution was performed with a binary gradient system at 1.0 mL/min flow rate using trifluoroacetic acid 0.1% in water as mobile phase (A) and trifluoroacetic acid 0.1% in acetonitrile as mobile phase (B). The elution profile was as follows: t = 0 %A = 100, %B = 0; from 0 to 10 min, linear gradient up to 100% B; from t = 10 min to t = 20 min %A = 0, %B = 100. Detection was accomplished with a 3"×3" NaI (Tl) crystal scintillation detector. Activity measurements were performed either in a Dose Calibrator, Capintec CRC-5R or in a scintillation counter, 3"×3" NaI (Tl) crystal detector associated to an ORTEC monochanel analyzer.

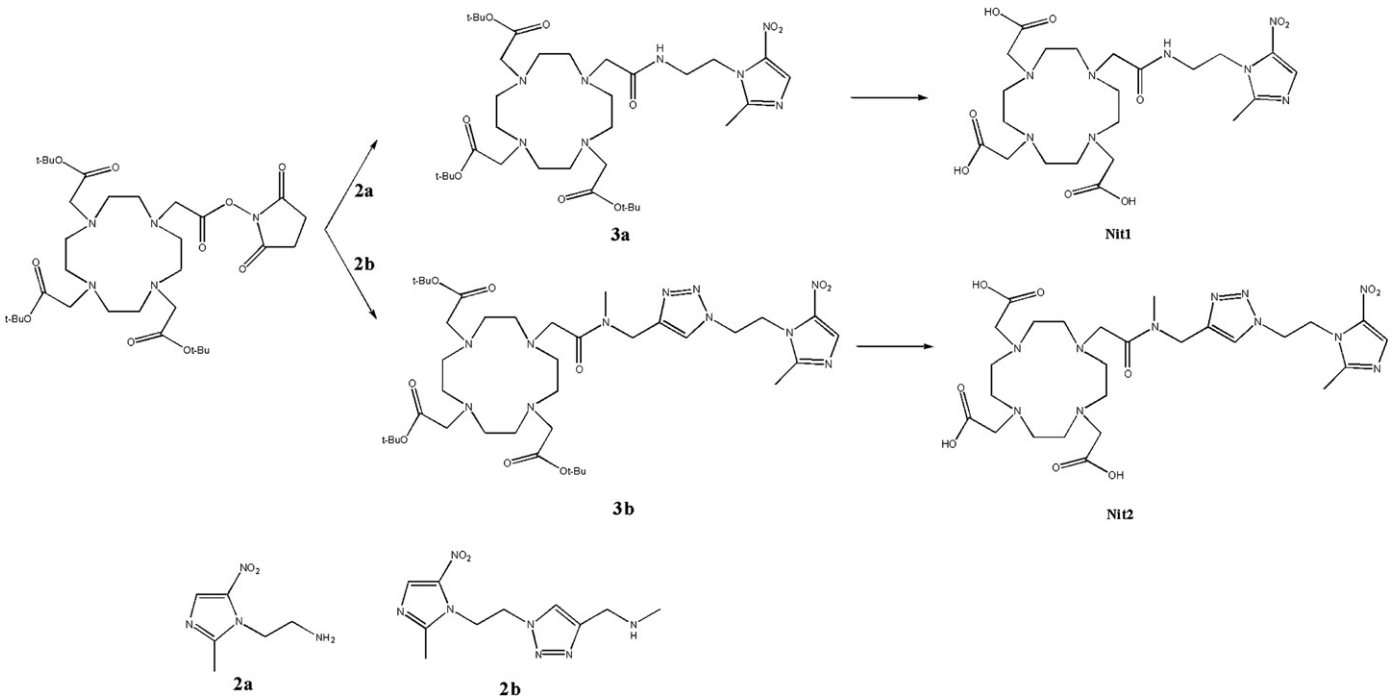

Scheme 1. Synthesis of ligands **Nit1** and **Nit2**.

2.2. Synthesis

2.2.1. Synthesis of Nit1

*2.2.1.1. 10-[2-(2-methyl-5-nitro-1 H-imidazole-1-yl)ethylaminocarbonylmethyl]-1,4,7-tris(tert-butoxycarbonylmethyl)-1,4,7,10-tetraazacyclododecane-1,4,7-acetate (**3a**).* A solution of the neutral amine **2a** (75 mmol) and *N*-hydroxisuccinimide-1,4,7-tris-(*tert*-butoxycarbonylmethyl)-1,4,7,10-tetraazacyclododecane-10-acetate [mono-NHS-tris-*t*-butyl-DOTA ester (**1**)] (75 mmol) in dried dichloromethane (3 mL) was stirred at room temperature during 4 days. Solvent was evaporated under reduced pressure and the final product was purified by chromatographic column (alumina) with a dichloromethane/methanol gradient as mobile phase. An oil product was obtained **3a** (47%). ^{1}H-RMN ($CDCl_3$) δ (ppm): 1.45 (m, 27 H, CH_3), 1.70–4.10 (bm + s, 29 H, CH_2, CH_3), 4.46 (t, J = 6.0 Hz, 2 H, $C\underline{H}_2$-NHCO), 6.81 (t, J = 6.4 Hz, 1 H, NH), 7.90 (s, 1 H, CH-imidazole). MS, *m/z* (abundance): 707 ($M^{+\bullet}$ - OH, 1%), 554 ($M^{+\bullet}$ - 170, 1%), 107 ($M^{+\bullet}$ - 617, 10%), 56 ($CH_2=C(CH_3)_2$, 57%), 41 ($CH_2=CHCH_3$, 100%), 28 ($CH_2=CH_2$, 19%).

2.2.1.2. **Nit1**. Desprotection of **3a** (29 nmol) was carried out with an excess of trifluoroacetic acid (0.60 mmol) in chloroform (2 mL) heated under reflux for 4 hours. After then, the solvent was evaporated under reduced pressure. ^{1}H-RMN (D_2O) δ (ppm): 2.60–4.40 (bm + s, 29 H, CH_2, CH_3), 4.55 (t, 2 H, $C\underline{H}_2$-NHCO), 8.35 (s, 1 H, CH).

2.2.2. Synthesis of Nit2

*2.2.2.1. Synthesis of 10-{[N-methyl-1-[1-(2-(2-methyl-5-nitro-1 H-imidazole-1-yl)ethyl)-1 H-1,2,3-triazole-4yl]methylaminocarbonylmethyl}-1,4,7,10-tetraazacyclododecane-1,4,7-acetate (**3b**).* A solution of amine **2b** (75 mmol) and *N*-hydroxisuccinimide-1,4,7-tris-(*tert*-butoxycarbonylmethyl)-1,4,7,10-tetraazacyclododecane-10-acetate (mono-NHS-tris-*t*-butyl-DOTA ester, **1**) (75 mmol) in dried dichloromethane (3 mL) was stirred at room temperature during 4 days. Solvent was evaporated under reduced pressure and the final product was purified by chromatographic column (alumina) with a dichloromethane/methanol gradient as mobile phase. An oil product was obtained **3b** (49%). ^{1}H-RMN ($CDCl_3$) δ (ppm): 1.46 (m, 27 H, CH_3), 1.80–3.70 (bm + 2 s, 32 H, CH_2, CH_3), 4.81 (m, 4 H, CH_2), 7.92 + 8.25 (2 s, 1 H, CH-triazole), 7.94 (s, 1 H, CH-imidazole). MS, *m/z* (abundance): 514 ($M^{+\bullet}$ - 315, 1%), 264 ($\mathbf{2b}^+$, 1%), 248 ($\mathbf{2b}^+$ - OH, 3%), 56 ($CH_2=C(CH_3)_2$, 75%), 41 ($CH_2=CHCH_3$, 100%), 28 ($CH_2=CH_2$, 42%).

2.2.2.2. **Nit2**. Desprotection of **3b** (29 nmol) was carried out with an excess of trifluoroacetic acid (0.60 mmol) in chloroform (2 mL) heated under reflux for 4 hours. After that, the solvent was evaporated under reduced pressure.

2.3. Radiolabelling

2.3.1. Preparation of [^{68}Ga]-complexes

A sodium acetate solution (1.14 M, 400 μL) was added to [^{68}Ga]$GaCl_3$ (1000–1500 MBq, 2.5 mL) to adjust pH to 4.5. Ligand **Nit1** or **Nit2**, (18–20 nmol) was added and the reaction mixture was incubated at 95 °C for 15 minutes. Radiochemical purity was controlled by HPLC (see 2.1).

2.3.2. Preparation of [^{18}F]fluoro-misonidazole

[^{18}F]FMISO was prepared, as described in [27], by nucleophilic fluorination of 1-(2′-nitro-1′-imidazolyl)-2-*O*-tetrahydropyranyl-3-*O*-toluenesulfonyl-propanediol (3.3 mg) for 10 min at 100 °C in acetonitrile (1 mL) followed by acidic hydrolysis of the protecting group with 1 M HCl (1 mL) for 5 min at 100 °C. Dilution with water: ethanol (95:5) (1 mL) and purification by HPLC (Nucleosil 100–7 C18 VP 250/16 Mancherey-Nagel column and ethanol/water 5:95; 4 mL/min, UV 220 nm, t_R = 29 min) provided pure [^{18}F]FMISO in 31 ± 5% non-decay-corrected radiochemical yield.

2.4. Physicochemical evaluation

2.4.1. Stability in labelling milieu

[^{68}Ga]-**Nit1** and [^{68}Ga]-**Nit2** were incubated in the labelling milieu at room temperature and the radiochemical purity was assessed by HPLC using chromatographic conditions described in 2.1. for up to 4 h after labelling.

2.4.2. Stability in plasma

[^{68}Ga]-**Nit1** and [^{68}Ga]-**Nit2** (100 μL) were incubated in human plasma (900 μL) at 37 °C for up to 2 h. After 30, 60 and 120 min incubation, samples (200 μL) were precipitated with ethanol (200 μL), centrifuged (12000 rpm, 5 min) and analysed by HPLC using chromatographic conditions described in 2.1.

2.4.3. DTPA challenge

[^{68}Ga]-**Nit1** and [^{68}Ga]-**Nit2** were incubated with excess of diethylene triamine pentaacetic acid (DTPA) in aqueous solution (100 molar-excess) at 37 °C and radiochemical purity of the gallium complexes was assessed by HPLC using chromatographic conditions described in 2.1 for up to 2 hours.

2.4.4. Lipophilicity

Lipophilicity was studied through the apparent partition coefficient between 1-octanol and phosphate buffer (0.125 M, pH 7.4). In a centrifuge tube, containing 2 mL of each phase, 0.1 mL of the [^{68}Ga]-complexes in solution were added, and the mixture was shaken on a Vortex mixer and finally centrifuged at 5000 rpm for 5 min. Three samples (0.2 mL) from each layer were counted in a gamma counter. The partition coefficient was calculated as the mean value of each cpm/mL of 1-octanol layer divided by that of the buffer. Lipophilicity was expressed as log P. Lipophilicity of [^{18}F]FMISO was determined using the same methodology.

2.4.5. Protein binding studies

[^{68}Ga]-**Nit1** and [^{68}Ga]-**Nit2** (25 μL) were incubated with human plasma (475μL) at 37 °C for up to 1 hour. At 30 and 60 min 50 μL samples were added to Microspin G-50 columns (Pharmacia Biotech), which have been pre-spun at 2000 g for 1 min. Columns were centrifuged again at 2000 g for 2 min and the collected eluate and the column were counted in a NaI-scintillation counter. Protein bound tracer was calculated as the percentage of activity eluted from the column.

2.5. Biological evaluation

2.5.1. Cell uptake studies

The cell culture studies were performed using the adherent cell line HCT-15 (CCL-255TM ATCC) corresponding to human adenocarcinoma. Cells were cultured in RPMI-1640 (R6504 Sigma-Aldrich) supplemented with 10% foetal bovine serum (Gibco), penicillin 100 U/mL (Sigma) and 100 g/mL streptomycin (Sigma) in T75 tissue culture flasks (Nunc, Denmark) at 37 °C and 5 % CO_2 until approximately 7.5×10^6 cells were obtained. Before the assay, flasks containing the cells were pre-incubated in a chamber gassed with N_2 for one hour to remove oxygen from the milieu. [^{18}F]FMISO and [^{68}Ga]-complexes were added and incubated for an additional period of 60 minutes. The same procedure was repeated in normal culture conditions (37 °C and 5 % CO_2) to use as control. After incubation time elapsed, culture milieu was removed, cells were washed with PBS and treated with Trypsin-EDTA (Sigma). Finally, activity in the supernatant and in the cells was measured in a solid scintillation counter and results were expressed as the ratio between the percentages of activity taken up by cells incubated in nitrogen (hypoxia) and incubated in normal conditions (normoxia).

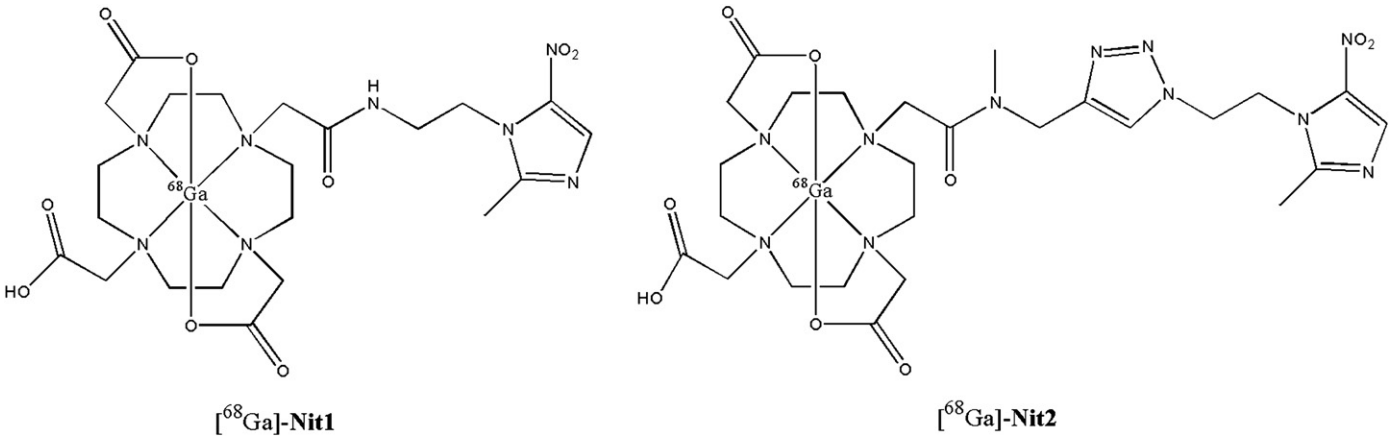

Fig. 1. Proposed structures for complexes [^{68}Ga]-**Nit1** and [^{68}Ga]-**Nit2**.

2.5.2. Animal studies

All animal studies were approved by the Ethics Committee of the Faculty of Chemistry from Uruguay.

2.5.2.1. Biodistribution in animals bearing induced tumours. A culture of 3LL Lewis murine lung carcinoma cells were expanded and treated with trypsine previous to inoculation. A cell suspension in PBS containing 3×10^6 cells was prepared and injected subcutaneously in the right limb of C57BL/6 mice (8–10 weeks old). 20–30 days later the animals developed palpable tumour nodules ($1.5\times0.5\times0.5$ cm) and were used for biodistribution studies.

Three animals per group were injected via a lateral tail vein with the [^{68}Ga]-compounds (0.1 mL, 0.037 – 0.37 MBq). At different intervals after injection the animals were sacrificed by neck dislocation. Whole organs and samples of blood and muscle were collected, weighed and assayed for radioactivity as well as tumours. Total urine volume was collected during the biodistribution period and also removed from bladder after sacrifice. The bladder, urine and intestines were not weighed. Corrections by different sample geometry were applied when necessary. Results were expressed as % dose/organ and % dose/g tissue.

3. Results and discussion

3.1. Synthesis of ligands

Synthesis of ligands **Nit1** and **Nit2** was achieved by reaction of the corresponding amino-derivative of metronidazole (**2a** or **2b**, respectively) with the mono-NHS-tris-*t*-butyl-DOTA ester **1**, followed by desprotection of the *tert*-butyl esters, as shown in Scheme 1. Ligand structures were designed using the following criteria: 1) Chelator unit retains at least two free carboxylate groups in order to coordinate gallium together with the four DOTA-nitrogens; 2) 5-nitroimidazo-1-yl moiety has been conjugated to a DOTA unit through two different linkers with different stereoelectronic behaviour. The aim was to study the influence of the linker on the final properties of the compounds, not only as a consequence of the linker structure but also for the formation of a secondary (**Nit1**) or tertiary (**Nit2**) amide bond between the chelator unit DOTA and the linker.

Synthesis yielded the desired products after chromatographic isolation. Structural characterization was performed by ^{1}H-NMR and mass spectrometry. Results were consistent with proposed structures.

3.2. Radiolabelling

DOTA is a tetraaza macrocyclic chelator which is widely used as bifunctional agent in ^{68}Ga-radiopharmaceutical development. Coordination of gallium occurs through the four nitrogen atoms and two carboxylic acid groups. The bioreductive moiety (5-nitroimidazole) was previously coupled to DOTA through an amide bond. Fig. 1 shows the proposed structure of [^{68}Ga]-complex with **Nit1** and **Nit2**.

Synthesis of the [^{68}Ga]-complexes was performed at pH 4.5 and 95 °C during 15 minutes. In both cases, HPLC revealed the formation of a single product with a retention time of 10.1 and 10.8 minutes for [^{68}Ga]-**Nit1** and [^{68}Ga]-**Nit2**, respectively, and radiochemical purity above 90% (Fig. 2).Specific radioactivity for both complexes was 67 ± 23 MBq/nmol of total ligand. The radioactivity recovery from the

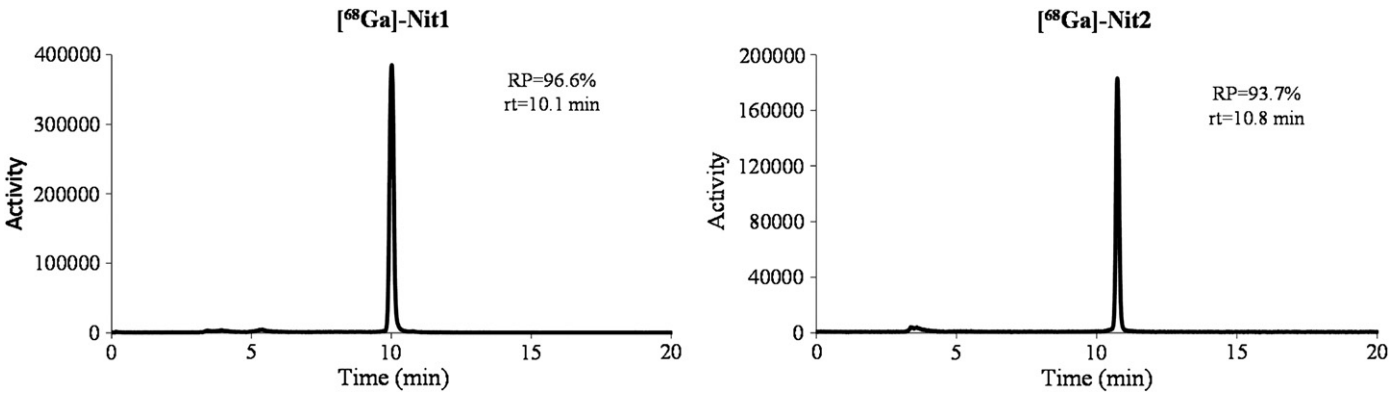

Fig. 2. Typical chromatograms for [^{68}Ga]-complexes (RP-HPLC eluted with trifluoroacetic acid 0.1% in water:trifluoroacetic acid 0.1% in acetonitrile (0 to 100%), coupled to γ-detector).

Table 1
Uptake of [^{68}Ga]-Nit1 and [^{68}Ga]-Nit2 both in normoxia and hypoxia.

Complex	Uptake hypoxia/normoxia (n = 3)
[^{68}Ga]-Nit1	3.27 ± 0.03
[^{68}Ga]-Nit2	2.03 ± 0.02
[^{18}F]FMISO (positive control)	2.30 ± 0.30

Values are shown as mean ± S.D.

column was monitored by means of an on-line solid scintillation detector coupled to the HPLC system and found to be quantitative.

3.3. Physicochemical evaluation

3.3.1. Stability studies

The complexes were stable for at least 4 h in labelling milieu. On the other hand, stability after incubation in human plasma for 2 h at 37 °C was also studied and found to be over 90%. Incubation of complexes with a 100-molar excess of DTPA showed high stability (100%) and no *trans*-chelation of the gallium.

3.3.2. Lipophilicity

The partition coefficient between 1-octanol and phosphate buffer pH 7.4 of the [^{68}Ga]-complexes was measured in order to assess its lipophilicity. A logP of −1.65 ± 0.05 and −3.30 ± 0.10 were obtained for [^{68}Ga]-**Nit1** and [^{68}Ga]-**Nit2**, respectively. These values are in agreement with the proposed structure of complexes since incorporation of a DOTA unit increases hidrophilicity of small molecules. Furthermore, a significant influence of the linker is observed in the lipophilicity, since the [^{68}Ga]-**Nit2**complex which bears a triazole unit in the linker has a lower logP value. A logP of −0.40 ± 0.03 was obtained for [^{18}F]FMISO using the same methodology. [^{68}Ga]-**Nit1** and [^{68}Ga]-**Nit2** are significantly more hydrophilic than [^{18}F]FMISO and this is a clear advantage considering that slow washout from normoxic tissues caused by excessive lipophilicity, is considered a serious drawback of this radiopharmaceutical.

3.3.3. Protein binding

Binding to plasma protein was studied using size exclusion chromatography. Ideally, low protein binding is required in order to ensure adequate pharmacokinetics of the potential radiopharmaceuticals. Additionally, only the unbound fraction of the radiotracer will penetrate cells and other biological membranes [28]. Low protein binding values were obtained for both complexes, 2.3 ± 0.1% for [^{68}Ga]-**Nit1** and 4.1 ± 0.2% for [^{68}Ga]-**Nit2**, correlating with the high *in vitro* stability and low lipophilicity of these complexes.

3.4. Biological evaluation

3.4.1. Cell uptake studies

In vitro uptake of [^{68}Ga]-**Nit1** and [^{68}Ga]-**Nit2** both in normoxia and hypoxia was evaluated using human colon adenocarcinoma HCT-15 cells in culture. Cells were incubated at 37 °C under an atmosphere of 95 % air plus 5 % carbon dioxide (aerobic exposure) or 95% nitrogen plus 5% carbon dioxide. According to literature oxygen concentration < 1000 ppm is considered hypoxic condition [29,30]. After 60 min equilibration period, the radiolabelled compounds were added and incubated with the cells for other 60 min. It has been shown by means of propidium iodide viability test [27] that HCT-15 cells maintain > 90% of viability for at least 90 minutes under the hypoxic conditions of this assay. Finally, cells were separated from supernatant and activity measured in order to compare the percentage taken up in normoxic and hypoxic conditions. This study has been previously validated by our group and used successfully in the evaluation of [^{99m}Tc]-complexes [22]. [^{18}F]FMISO was used as a positive control. Both complexes showed preferential uptake in hypoxia, as shown in Table 1. The ratio of uptake in hypoxia/normoxia was in the same range or even higher in comparison to [^{18}F]FMISO. Furthermore, [^{68}Ga]-**Nit1** displayed a 1.5-fold higher ratio than the positive control, a value that was significantly higher than the [^{68}Ga]-**Nit2** complex.

3.4.2. Biodistribution in animals bearing induced tumours

Biodistribution studies were carried out in C57 mice bearing induced Lewis carcinoma. This animal model was selected because histopathologic studies demonstrated high degree of hypoxia within the tumours [22]. Table 2 shows the results expressed as percent dose per organ in the most significant organs as a function of time.

[^{18}F]FMISO was evaluated in the same animal model and used for comparison (Table 3). Biological behaviour of the novel [^{68}Ga]-complexes was characterized by low blood and liver activity, rapid depuration and quantitative excretion through the urinary tract (91.4 ± 0.4% injected dose for [^{68}Ga]-**Nit1** and 86.1 ± 8.0% for [^{68}Ga]-**Nit2**, respectively, at 2 hours post-injection), as expected for highly hydrophilic compounds. Activities in other organs and tissues were negligible. Biodistribution results of [^{18}F]FMISO in the same animal model showed remarkably higher liver, lung and muscle uptake, as well as combined excretion through the urinary (24.0 ± 6.0% injected dose at 2 h) and hepatobiliary (22.26 ± 0.79% injected dose at 2 h) tract as expected for a compound with intermediate lipophilicity.

Table 4 summarizes *in vivo* tumour uptake (expressed as % Dose/g) as well as tumour/blood and tumour/muscle ratios for [^{68}Ga]-complexes.

Uptake of [^{68}Ga]-**Nit1** and [^{68}Ga]-**Nit2** in tumour was moderate (approx. 1 %/g at 30 minutes post-injection) and similar for both compounds. However, retention in tumour is significantly different;

Table 2
% Dose organ^{-1} in most significant organs as a function of time.

Organ	[^{68}Ga]-Nit1, % Dose organ^{-1} (n = 3)			[^{68}Ga]-Nit2, % Dose organ^{-1} (n = 3)		
	0.5 h	1 h	2 h	0.5 h	1 h	2 h
Blood	4.1 ± 1.9	1.89 ± 0.75	0.34 ± 0.07	2.7 ± 1.4	0.98 ± 0.07	1.66 ± 0.78
Liver	1.11 ± 0.20	0.68 ± 0.25	0.22 ± 0.06	1.21 ± 0.23	0.57 ± 0.07	0.69 ± 0.04
Heart	0.22 ± 0.15	0.06 ± 0.02	0.02 ± 0.01	0.16 ± 0.05	0.03 ± 0.01	0.05 ± 0.01
Lung	0.29 ± 0.07	0.12 ± 0.06	0.04 ± 0.02	0.22 ± 0.13	0.06 ± 0.01	0.09 ± 0.04
Spleen	0.09 ± 0.02	0.05 ± 0.03	0.02 ± 0.01	0.09 ± 0.03	0.02 ± 0.01	0.03 ± 0.01
Kidneys	1.67 ± 0.95	0.94 ± 0.21	0.47 ± 0.09	1.25 ± 0.50	2.11 ± 0.57	2.20 ± 0.71
Muscle	2.98 ± 0.78	2.03 ± 0.29	0.52 ± 0.21	3.73 ± 1.84	0.99 ± 0.19	1.25 ± 0.26
Tumour	1.31 ± 0.93	1.31 ± 0.64	0.70 ± 0.25	1.34 ± 0.55	0.81 ± 0.05	3.39 ± 0.24
Stomach	0.33 ± 0.26	0.05 ± 0.01	0.07 ± 0.04	0.12 ± 0.06	0.12 ± 0.01	0.08 ± 0.05
Intestine	1.28 ± 0.54	1.02 ± 0.13	0.47 ± 0.07	1.12 ± 0.31	0.56 ± 0.10	1.08 ± 0.37
Bladder + urine	87.4 ± 5.2	78.0 ± 9.8	91.4 ± 0.4	85.9 ± 6.0	91.6 ± 1.6	86.1 ± 8.0

Values are shown as mean ± S.D.

Table 3
% Dose organ^{-1} in organs as a function of time.

Organ	[^{18}F]FMISO, % Dose organ^{-1} ($n=3$)		
	0.5 h	1 h	2 h
Blood	3.56 ± 0.43	2.95 ± 0.36	0.95 ± 0.06
Liver	8.7 ± 1.6	6.60 ± 0.42	3.4 ± 1.3
Heart	0.28 ± 0.04	0.23 ± 0.03	0.08 ± 0.04
Lung	0.52 ± 0.05	0.44 ± 0.06	0.18 ± 0.10
Spleen	0.27 ± 0.07	0.17 ± 0.01	0.07 ± 0.02
Kidneys	1.68 ± 0.85	1.42 ± 0.60	0.44 ± 0.19
Muscle	13.35 ± 0.64	11.9 ± 2.2	2.7 ± 1.0
Tumour	4.28 ± 0.54	4.1 ± 2.1	2.6 ± 1.3
Stomach	0.73 ± 0.12	0.58 ± 0.06	0.35 ± 0.19
Intestine	17.5 ± 2.5	21.8 ± 3.5	22.26 ± 0.79
Bladder + urine	14.2 ± 3.9	17.1 ± 4.9	24.0 ± 6.0

Values are shown as mean ± S.D.

while 50% of the initial activity is cleared from tumour in 2 hours for [^{68}Ga]-**Nit1**, almost 100% of the dose taken up is retained after 2 hours for [^{68}Ga]-**Nit2**.

Behaviour of [^{18}F]FMISO (Table 5) was similar to that of [^{68}Ga]-**Nit2** (aprox. 100% of retention in tumour) but with a significantly higher uptake ($p>0.05$) in tumour at all-time points, probably due to better cell penetration of a more lipophilic compound.

Soft tissue clearance of gallium compounds was fast due to their high hidrophilicity and this was reflected in tumour/muscle ratios, which are very favourable during all the studied period for both gallium complexes, (5.1 ± 1.7 and 6.6 ± 1.6 at 2 h, for [^{68}Ga]-**Nit1** and [^{68}Ga]-**Nit2**, respectively). [^{18}F]FMISO, on the other hand, showed a significantly higher initial muscle uptake and slower depuration, as expected from bibliographic data that indicate slow depuration rates from blood and soft tissues as the main disadvantages of this radiopharmaceutical.

The comparative statistical analysis demonstrated that our [^{68}Ga]-complexes showed significantly higher tumour/muscle ratios at all-time points ($p<0.05$) (Table 4). After 60 min of injection, [^{68}Ga]-**Nit1** displayed near to 1.7-fold higher tumour/muscle ratio than [^{18}F]FMISO while [^{68}Ga]-**Nit2** exhibited near to 2.7-fold higher ratio than the positive control radiopharmaceutical.

Blood activity showed a different pattern for [^{68}Ga]-**Nit1** and [^{68}Ga]-**Nit2**: [^{68}Ga]-**Nit1** had higher initial blood activity but a very fast depuration, while dose/g in blood for [^{68}Ga]-**Nit2** was lower at 30 minutes post-injection but demonstrated negligible depuration. These results lead to initial tumour/blood ratios below 1 for both [^{68}Ga]-**Nit1** and [^{68}Ga]-**Nit2**. Although ratios increased at longer biodistribution times, statistical analysis demonstrated that activity in tumour was not significantly higher than activity in blood at any time point ($p>0.05$).

Activity in blood followed a similar profile also in [^{18}F]-MISO: relatively high initial dose/g in blood and slow depuration. Uptake in tumour for [^{18}F]FMISO was also not statistically significantly ($p>0.05$) higher than in blood.

Table 5
Tumour uptake (expressed as % dose g^{-1}).

Organ	[^{18}F]FMISO, % Injected dose g^{-1} ($n=3$)		
	0.5 h	1 h	2 h
% Tumour g^{-1}	3.45 ± 0.85	3.25 ± 0.66	2.0 ± 1.2
% Blood g^{-1}	2.46 ± 0.52	2.18 ± 0.12	0.67 ± 0.05
% Muscle g^{-1}	1.50 ± 0.23	1.32 ± 0.21	0.30 ± 0.12
Tumour/muscle ratio	2.29 ± 0.21	2.52 ± 0.76	4.4 ± 1.0
Tumour/blood ratio	1.40 ± 0.15	1.37 ± 0.24	2.9 ± 1.6

Values are shown as mean ± S.D.

In conclusion, these results indicate that [^{68}Ga]-**Nit1** and [^{68}Ga]-**Nit2** exhibit promising biological behaviour as potential agents for hypoxia imaging in hypoxic tumours. In spite of differences in physicochemical parameters between these two complexes, no significant differences were observed in biological behaviour. Their advantage in comparison with [^{18}F]FMISO is a higher hidrophilicity and a faster soft clearance depuration. On the other hand, tumour uptake and retention is significantly lower than that of [^{18}F]FMISO. Kinetics in blood has neither advantages nor disadvantages in comparison with the gold standard.

Although many nitroimidazole derivatives labelled with different radionuclides have been evaluated as potential hypoxia targeting agents, their comparison is difficult due to both the heterogeneity in animal models used and nature of the tumours. Furthermore, no comparison with [^{18}F]FMISO in the same experimental conditions has been reported to our knowledge. Analysis of previously reported data, including some of our own research group, showed that tumour uptake of [^{68}Ga]-**Nit1** and [^{68}Ga]-**Nit2** was in the same order or even higher than other proposed hypoxia imaging agents [21–26,31].

These results indicate that [^{68}Ga]-**Nit1** and [^{68}Ga]-**Nit2** exhibit promising biological behaviour as potential agent for hypoxia imaging in hypoxic tumours.

4. Conclusions

This paper presents the development of two novel 5-nitroimidazole derivatives and the corresponding [^{68}Ga]-complexes, [^{68}Ga]-**Nit1** and [^{68}Ga]-**Nit2**, as potential radiopharmaceuticals for hypoxia PET imaging. *In vitro* and *in vivo* results have been compared to that of the gold standard for hypoxia imaging [^{18}F]FMISO in exactly the same experimental conditions and biological models. Influence of the linker structure was also studied.

Nit1 and **Nit2** ligands were obtained in good yields and structural characterization was made by NMR spectroscopy and mass spectrometry. Labelling was achieved with high radiochemical purity and both complexes resulted stable in labelling milieu and in human plasma, and did not show *trans*-chelation in the presence of the challenging ligand DTPA.

Gallium compounds were significantly less lipophilic than the reference compound [^{18}F]FMISO thus overcoming the main

Table 4
Tumour uptake (expressed as % dose g^{-1}).

Organ	[^{68}Ga]-Nit1, % Injected dose g^{-1} ($n=3$)			[^{68}Ga]-Nit2, % Injected dose g^{-1} ($n=3$)		
	0.5 h	1 h	2 h	0.5 h	1 h	2 h
% Tumour g^{-1}	1.11 ± 0.46	0.84 ± 0.26	0.38 ± 0.16	1.05 ± 0.32	0.87 ± 0.23	1.19 ± 0.51
% Blood g^{-1}	3.2 ± 1.3	1.24 ± 0.41	0.25 ± 0.06	1.87 ± 0.86	0.72 ± 0.01	1.28 ± 0.51
% Muscle g^{-1}	0.46 ± 0.26	0.22 ± 0.02	0.09 ± 0.03	0.41 ± 0.20	0.13 ± 0.01	0.19 ± 0.11
Tumour/muscle ratio	2.47 ± 0.98	4.26 ± 0.54	5.1 ± 1.7	2.89 ± 0.91	6.8 ± 1.8	6.6 ± 1.6
Tumour/blood ratio	0.30 ± 0.08	0.70 ± 0.21	1.41 ± 0.46	0.61 ± 0.19	1.21 ± 0.33	1.18 ± 0.18

Values are shown as mean ± S.D.

disadvantage of this compound. *In vitro* binding studies demonstrated selectivity towards hypoxic tissue for both gallium compounds. Furthermore, the ratio of uptake in hypoxia/normoxia of [^{68}Ga]-**Nit1** was even higher than that of [^{18}F]FMISO indicating selective uptake in hypoxic conditions.

The overall biodistribution profile in mice was more favourable, especially because of the lower liver uptake, muscle and lung uptake, higher blood clearance and quantitative urinary excretion. However, uptake in tumour was also lower.

Another key feature of our gallium compounds is the more favourable tumour/muscle ratios, as a consequence of the higher hidrophilicity and faster depuration from soft tissues. In spite of differences in physicochemical parameters between these two complexes, no significant differences were observed in biological behaviour.

In conclusion, our gallium compounds have overcome the major disadvantage of [^{18}F]FMISO, namely, high lipophilicity and slow kinetics, and have demonstrated selective uptake in hypoxia. [^{18}F]FMISO remains superior in terms of tumour uptake. However, some authors claim that by introducing a second bioreductive centre in the molecule a higher selective localization in tumour hypoxia can be achieved [28]. Application of this strategy can be a valuable tool for increasing tumour uptake.

Acknowledgments

We thank Dr. M. Moreno and Dr. H. Balter for their collaboration. We also thank PEDECIBA-Química and ANII for scholarships to S. Fernández, and Gramón-Bagó S.A. for providing metronidazole.

References

[1] Caramelo P, Peña J, Castilla A, Justo S, De Solís AJ, Neira F, et al. Respuesta a la hipoxia. Medicina 2006;66:155.
[2] Nunn A, Linder K, Strauss HW. Nitroimidazoles and imaging hypoxia: a review. Eur J Nucl Med 1995;22:265-80.
[3] Liu R, Kiess MC, Okada RD, Block PC, Strauss HW, Pohost GM, et al. The persistent defect on exercise thallium imaging and its fate after myocardial revascularization: does it represent scar or ischemia? J Am Heart Assoc 1985;110:996.
[4] Straub NC. Transport of oxygen and carbon dioxide tissue oxygenation3rd. ed. . St. Louis: Mosby Yearbook; 1993.
[5] Buxton RB, Alpert NM, Babikian V, Weise S, Correia JA, Ackerman RH. Evaluation of the $^{11}CO_2$ positron emission tomographic method for measuring brain pH changes measured in states of altered pCO_2. J Cereb Blood Flow Metab 1987;7:709-19.
[6] Olive PL, Durand RE. Misonidazole binding in SCCVII tumours in relation to the tumour blood supply. Int J Rad Onc Biol Phys 1989;16:755-61.
[7] Connet RJ, Honig CG, Gayeski E, Brooks GA. Defining hypoxia: a systems view of VO_2, glycolysis, energetic and intracellular PO_2. J Appl Phys 1990;68:833-42.
[8] Kabayashi M, Nakagawa K. Metastasis and hypoxia-inducible factor. Gan To Kagaku Ryoho 2010;37:2047-51.
[9] Brizel DM, Scully SP, Harrelson JM, Layfield LJ, Bean JM, Prosnitz LR, et al. Tumor oxygenation predicts for the likelihood of distant metastases in human soft tissue sarcoma. Cancer Res 1996;56:941-3.
[10] Gray LH, Conger AD, Ebert M, Hornsey S, Scott OC. The concentration of oxygen dissolved in tissues at the time of irradiation as a factor in radiotherapy. Br J Radiol 1953;26:638-48.
[11] Vaupel P, Mayer A. Hypoxia in cancer: significance and impact on clinical outcome. Cancer Metastasis Rev 2007;26:225-39.
[12] Mukai T, Suwada J, Sano K, Okada M, Yamamoto F, Maeda M. Designed of Ga-DOTA-based bifunctional radiopharmaceuticals: two functional moieties can be conjugated to radiogallium-DOTA without reducing the complex stability. Bioorg Med Chem 2009;17:4285-90.
[13] Lee ST, Scott AM. Hypoxia positron emission tomography imaging with ^{18}F-fluoromisonidazole. Semin Nucl Med 2007;37:451-61.
[14] Bourgeois M, Rajerison H, Guerard F, Mougin-Degraef M, Barbet J, Michel N, et al. Nucl Med Rev Cent East Eur 2011;14:90-5.
[15] Chitneni SK, Palmer GM, Zalutsky MR, Dewhirst MW. Molecular imaging of hypoxia. J Nucl Med 2011;52:165-8.
[16] Takasawa M, Moustafa RR, Baron JC. Applications of nitroimidazole in vivo hypoxia imaging in ischemic stroke. Stroke 2008;39:1629-37.
[17] Hoigebazar L, Jeong JM. Hypoxia imaging agents labeled with positron emitters. Rec Res Can Res 2012;194:285-99.
[18] Hoigebazar L, Jeong JM, Choi SY, Choi JY, Shetty D, Lee YS, et al. Synthesis and characterization of nitroimidazole derivatives for ^{68}Ga-Labeling and testing in tumor xenografted mice. J Med Chem 2010;53:6378-85.
[19] Hoigebazar L, Jeong JM, Hong MK, Kim YJ, Lee JY, Shetty D, et al. Synthesis of ^{68}Ga-labeled DOTA-nitroimidazole derivatives and their feasibilities as hypoxia imaging PET tracers. Bioorg Med Chem 2011;19:2176-81.
[20] Cerecetto H, González M, Lavaggi ML. Development of hypoxia selective cytotoxins for cancer treatment: an update. Med Chem 2006;2:315-27.
[21] Cerecetto H, González M, Onetto S, Risso M, Rey A, Giglio J, et al. Synthesis and characterization of thiol containing furoxan derivatives as coligands for the preparation of potential bioreductive radiopharmaceuticals. Arch Pharm 2006;339:59-66.
[22] Giglio J, Rey A, Cerecetto H, Pirmettis I, Papadopoulos M, León E, et al. Design and evaluation of "3+1" mixed ligand oxorhenium and oxotechnetium complexes bearing a nitroaromatic group with potential application in nuclear medicine oncology. Eur J Med Chem 2006;41:1144-52.
[23] Giglio J, Patsis G, Pirmettis I, Papadopoulos M, Raptopoulou C, Pelecanou M, et al. Preparation and characterization of technetium and rhenium tricarbonyl complexes bearing the 4-nitrobenzyl moiety as potential bioreductive diagnostic radiopharmaceuticals. In vitro and in vivo studies. Eur J Med Chem 2008;43:741-8.
[24] Giglio J, Fernández S, Rey A, Cerecetto H. Synthesis and biological characterization of novel dithiocarbamate containing 5-nitroimidazole ^{99m}Tc-complexes as potential agents for targeting hypoxia. Bioorg Med Chem Lett 2011;21:394-7.
[25] Fernández S, Giglio J, Cerecetto H, Rey A. Influence of ligand denticity on the properties of novel ^{99m}Tc(I)–carbonyl complexes. Application to the development of radiopharmaceuticals for imaging hypoxic tissue. Bioorg Med Chem 2012;20:4040-8.
[26] Giglio J, Fernández S, Pietzsch H-J, Dematteis S, Moreno M, Pacheco JP, et al. Synthesis, in vitro and in vivo characterization of novel ^{99m}Tc-'4+1'-labeled 5-nitroimidazole derivatives as potential agents for imaging hypoxia. Nucl Med Biol 2012;39:679-86.
[27] Suzuki T, Fujikura K, Higashiyama T, Takata K. DNA staining for fluorescence and laser confocal microscopy. J Histochem Cytochem 1997;45:49-53.
[28] Huang H, Mei L, Chu T. Synthesis, radiolabeling and biological evaluation of propylene amine oxime complexes containing nitrotriazoles as hypoxia markers. Molecules 2012;17:6808-20.
[29] Lewis S, Welch MJ. PET imaging of hypoxia. Q J Nucl Med 2001;45:183-8.
[30] Nunn A, Linder K, Strauss HW. Nitroimidazoles and imaging hypoxia. Eur J Nucl Med 1995;22:265-80.
[31] Lim JL, Berridge MS. An efficient radiosynthesis of [^{18}F]fluoromisonidazole. Appl Radiat Isot 1993;44:1085-91.